Waves in Random and Complex Media
Vol. 00, No. 00, July 2009, 1–30

RESEARCH ARTICLE

Fractional Precursors in Random Media

Josselin Garnier[a*] and Knut Sølna[b]

[a]*Laboratoire de Probabilités et Modèles Aléatoires & Laboratoire Jacques-Louis Lions, Université Paris VII, 2 Place Jussieu, 75251 Paris Cedex 05, France*
Tel: (33).144.278.693 Fax: (33).144.277.650 Email: garnier@math.jussieu.fr
[b]*Department of Mathematics, University of California, Irvine CA 92697*
Tel: 949.824.3154 Fax: 949.824.7993 Email: ksolna@math.uci.edu

(*July 16, 2009*)

When a broadband pulse penetrates into a dissipative and dispersive medium, phase dispersion and frequency-dependent attenuation alter the pulse in a way that results in the appearance of a precursor field with an algebraic decay. We derive here the existence of precursors in non-dispersive, non-dissipative, but randomly heterogeneous and multiscale media. The shape of the precursor and its fractional power law decay with propagation distance depend on the random medium class. Three principal scattering precursor classes can be identified : (i) In exponentially decorrelating random media, and more generally in mixing random media, the precursor has a Gaussian shape and a peak amplitude that decays as the square root of the inverse of the propagation distance. (ii) In short-range correlation media, with rough multiscale medium fluctuations, the precursor has a skewed shape with a tail that exhibits an anomalous power law decay in time and a peak amplitude that exhibits an anomalous power law decay with propagation distance, both of which depend on the Hurst exponent that characterizes the roughness of the medium. (iii) In long-range correlation media with long-range memory, the situation mimics that of class (ii), but with modified power laws.

Keywords: Random media, mutliscale media, steepest descent, precursor.

1. Introduction

Heterogeneous and multiscale media play an important role in many different application areas, such as in geophysics [9] or in laser beam propagation through the atmosphere [12, 26]. Due to multiple scattering pulse propagation is then characterized by a random time shift described in terms of a fractional Brownian motion and a deterministic spreading described by a pseudo-differential operator. This operator is characterized by a frequency-dependent attenuation that obeys a power law with an exponent ranging from 0 to 2 that is related to the fractal (or Hurst) parameter of the multiscale medium. This frequency-dependent attenuation is associated with a frequency-dependent phase, which ensures causality and that the Kramers-Kronig relation is satisfied. In the time domain the effective wave equation has the form of a linear integro-differential equation with a fractional derivative. These results are derived in [14]. Related results for particular situations, respectively paraxial propagation, strongly heterogeneous media with long-range correlations and Goupillaud media can be found in [10, 21, 29]. In [28] the transmitted pulse in so called locally layered media was considered and it was shown that central results on the pulse deformation are robust with respect to such medium perturbations,

*Corresponding author.

ISSN: 0278-1077 print/ISSN 1745-5049 online
© 2009 Taylor & Francis
DOI: 10.1080/1745503YYxxxxxxxx
http://www.informaworld.com

while in [13] solitons in random media with long range perturbations was considered and it was shown that aspects of the pulse deformation theory that predicts power law rather than exponential decay generalizes to nonlinear situations.

On the other hand it is known that, when a broadband pulse penetrates into a causally dispersive medium, the interrelated effects of phase dispersion and frequency dependent attenuation alter the pulse in a way that results in the appearance of a precursor field with a nonexponential decay. Precursors have been studied for a long time in homogeneous media [4, 7, 30], in which the amplitude of the precursor decays as the square root of the inverse of the propagation distance. Early experimental observations of "Brillouin" precursors involved microwaves in waveguides [25]. Experimental studies have been carried out also in the optical regime exploring the prospect of utilizing them for study of materials and biological systems [1, 27]. Motivated in part by potential applications to for instance radar technology, remote sensing, communications and information technology researchers continue to explore the role of precursors [17–20, 22, 23]. In the context of microwave exposure of tissue the role of precursors has been studied in [2, 3]. A central motivation in these studies is the algebraic and slow decay of the precursor, as the square root of the inverse of the propagation distance in the classic case.

In this paper we study the long-distance propagation of a step function modulated sine wave in a multiscale medium and the emergence of a special precursor from the effective fractional wave equation. We will in particular see that the precursor has a power law decay rate, with a fractional exponent that is related to the Hurst parameter of the multiscale random medium. Thus, we shall refer to these precursors occurring in "fractal" like or multiscale media as *fractional precursors*. Their behaviors are similar to the classic precursors of homogeneous dispersive media, however, they occur under very different circumstances since effective dispersion and attenuation result from multiple scattering in a medium whose components are not dissipative neither dispersive.

The outline of the paper is as follows. First, we give some background on the analytic framework for analysis of waves in one-dimensional random media in Sections 2 to 4. The analysis of the precursor will be based on a fractional effective equation for the transmitted wave in multiscale media that we recapitulate in Section 4. Then we discuss the results regarding the fractional precursor in Section 5 and we derive these results in Section 6. Technical parts of the proofs are given in the appendices.

2. Modeling of Waves in Complex Environments

We consider the one-dimensional wave equation in the presence of random fluctuations of the medium:

$$\frac{\partial^2 p}{\partial z^2} - \frac{n^2(z)}{c_0^2}\frac{\partial^2 p}{\partial t^2} = F(t,z)\,. \tag{1}$$

Here $p(t,z)$ is the pressure field in acoustics or the electric field in electromagnetics and in optics. The speed of propagation in the homogeneous background medium is c_0 and the index of refraction of the medium $n(z)$ is assumed to be randomly varying. We assume that the source $F(t,z)$ is located at 0 and emits a right-going signal starting at time 0.

We consider the weakly heterogeneous regime [11] in which the index of refraction has small and rapid fluctuations (compared to the propagation distance). We write

it in the form

$$n^2(z) = 1 + \nu(z)\,.$$

The random process $\nu(z)$ is assumed to be stationary and to have mean zero. Its autocorrelation function is denoted by

$$\phi(z) := \mathbb{E}[\nu(x)\nu(x+z)]\,, \tag{2}$$

where $\mathbb{E}$ stands for the expectation with respect to the distribution of the random medium. The function $\phi(z)$ is bounded, even, and maximal at zero ($\phi(0)$ is the variance of the fluctuations). Its local properties at zero and its asymptotic behavior at infinity characterize the short- and long-range correlations of the random medium, as we discuss in the next section.

3. Regimes of Clutter

Wave propagation in random media is usually studied with a driving process ν that has mixing properties. This means that the random values $\nu(x+z)$ and $\nu(x)$ taken at two points separated by the distance z become rapidly uncorrelated when $z \to \infty$. In other words the autocorrelation function $\phi(z)$ decays rapidly to zero as $z \to \infty$. More precisely we say that the random process ν is mixing if its autocorrelation function decays fast enough at infinity so that it is absolutely integrable:

$$\int_0^\infty |\phi(z)|dz < \infty\,. \tag{3}$$

This is the usual assumption for random media, under which the theory is well established. In this case the correlation length can be defined as $l_c = 2\int_0^\infty \phi(z)dz/\phi(0)$. The standard O'Doherty-Anstey (ODA) theory describes the propagating pulse in this regime. The effective equation for the wave front has been obtained by several authors [5, 6, 8, 11]. The pulse propagation is characterized by a random time shift and a deterministic spreading. The random time shift is described in terms of a standard Brownian motion, while the deterministic spreading is described by a pseudo-differential operator that we will discuss in Section 4.

Wave propagation in multiscale and rough media, with short- or long-range fluctuations, has recently attracted a lot of attention (as mentioned in the introduction). Examples are given in [14] and the effective pulse propagation in multiscale and rough media is described in Section 4.

Qualitatively, the long-range correlation property means that the random process has long memory (in contrast to a mixing process). This means that the correlation degree between the random values $\nu(x+z)$ and $\nu(x)$ taken at two points separated by the distance z is not completely negligible when $z \to \infty$. It corresponds to the fact that the autocorrelation function has a slow decay at infinity. More precisely we say that the random process ν has the H-long-range correlation property if its autocorrelation function satisfies:

$$\phi(z) \overset{|z|\to\infty}{\simeq} r_H \Big|\frac{z}{l_c}\Big|^{2H-2} + o\Big(\Big|\frac{z}{l_c}\Big|^{2H-2}\Big)\,, \tag{4}$$

where $r_H > 0$ and the *Hurst parameter* $H \in (1/2, 1)$. Here the correlation length l_c

is the critical length scale beyond which the power law behavior (4) is valid. Note that the autocorrelation function is not integrable since $2H-2 \in (-1,0)$, which means that a random process with the H-long-range correlation property is not mixing. Additional technical hypotheses on the random process ν are required for the derivation of the effective fractional wave equation and they are given in [14].

Qualitatively the short-range correlation property means that the random process is rough at small scales. This means that the correlation degree between the random values $\nu(x+z)$ and $\nu(x)$ taken at two points separated by the distance z has a sharp decay at zero. It corresponds to the fact that the autocorrelation function decays faster than an affine function at zero. More precisely we say that the random process ν has the H-short-range correlation property if its autocorrelation function satisfies:

$$\phi(z) \overset{|z|\to 0}{\simeq} \phi(0)\Big(1 - d_H\Big|\frac{z}{l_c}\Big|^{2H} + O\Big(\Big|\frac{z}{l_c}\Big|\Big)\Big)\,, \tag{5}$$

where $d_H > 0$ and $H \in (0,1/2)$. Here the correlation length l_c is the critical length scale below which the power law behavior (5) is valid.

4. Random Effective Propagation Model

In Ref. [14] we studied the pulse propagation through random media with mixing, long-range, and short-range correlation properties, in the weakly scattering regime (small-amplitude medium fluctuations and large propagation distance). We have found in [14] that the right-going pulse

$$a(\tau, z) = p\big(\tau_0(z) + \tau, z\big)$$

in the frame moving with the random travel time

$$\tau_0(z) = \frac{z}{c_0} + \frac{1}{2c_0}\int_0^z \nu(x)dx$$

(whose statistics for large propagation distances can be described in terms of a fractional Brownian motion in the long- and short-range cases) has the deterministic form

$$a(\tau, z) = \frac{1}{2\pi}\int \exp\Big(-i\omega\tau - \frac{\gamma_c(\omega)\omega^2}{8c_0^2}z - i\frac{\gamma_s(\omega)\omega^2}{8c_0^2}z\Big)\hat{f}(\omega)d\omega\,, \tag{6}$$

where $\hat{f}(\omega)$ is the Fourier transform of the initial pulse and

$$\gamma_c(\omega) := 2\int_0^\infty \phi(z)\cos\Big(\frac{2\omega z}{c_0}\Big)dz\,, \tag{7}$$

$$\gamma_s(\omega) := 2\int_0^\infty \phi(z)\sin\Big(\frac{2\omega z}{c_0}\Big)dz\,. \tag{8}$$

The pulse profile $a(\tau, z)$ satisfies the partial differential equation (PDE):

$$\frac{\partial a}{\partial z} = \mathcal{L}a\,, \tag{9}$$

where $\mathcal{L}$ is a pseudo-differential operator that describes the deterministic pulse deformation:

$$\mathcal{L} = \mathcal{L}_c + \mathcal{L}_s \,, \tag{10}$$

$$\int_{-\infty}^{\infty} \mathcal{L}_c a(\tau) e^{i\omega\tau} d\tau = -\frac{\gamma_c(\omega)\omega^2}{8c_0^2} \int_{-\infty}^{\infty} a(\tau) e^{i\omega\tau} d\tau \,, \tag{11}$$

$$\int_{-\infty}^{\infty} \mathcal{L}_s a(\tau) e^{i\omega\tau} d\tau = -\frac{i\gamma_s(\omega)\omega^2}{8c_0^2} \int_{-\infty}^{\infty} a(\tau) e^{i\omega\tau} d\tau \,. \tag{12}$$

The PDE (9) is completed with the initial condition $a(\tau, z = 0) = f(\tau)$ corresponding to the initial pulse profile. The above results derive from averaging in certain integro-differential equations that describes the evolution of the front shape with the propagation distance z and is based on an asymptotic scaling mentioned above, see [14] for the details. We remark here that the pulse $a(\tau, z)$ corresponds to observing the wave field at position z when centered in time at a *random time* $\tau_0(z)$. The random centering of the observation window can be described precisely. Let $\tau(z)$ be the first arrival time at position z, that is, the integral of the reciprocal of the local speed of sound in between the surface $z = 0$ and the observation point z. Then we have in the asymptotic framework presented in [14]:

$$\tau_0(z) - \tau(z) \simeq \frac{z\phi(0)}{8c_0} \,. \tag{13}$$

Note therefore that to leading order we have a deterministic delay relative to the first arrival time, the scattering gradually delays the pulse, while the random arrival time τ_0 itself can be described in distribution in terms of a zero-mean standard or fractional Brownian motion process with respect to the spatial variable.

The first qualitative property satisfied by the pseudo-differential operator $\mathcal{L}$ is that it is non-local (in the time domain) but it preserves the causality. Indeed we can write

$$\mathcal{L}a(\tau) = \frac{1}{8c_0} \int_0^{\infty} \phi\left(\frac{c_0 s}{2}\right) \frac{\partial^2 a}{\partial \tau^2}(\tau - s) ds \,. \tag{14}$$

Equation (9) gives the effective evolution of the front wave $a(\tau, z)$ in the frame moving with the random travel time $\tau_0(z)$. If we ignore the small random time shift and focus our attention to the deterministic pulse deformation, then we can write the effective equation in the form of a wave equation for the wave field in the original frame as:

$$\begin{aligned} &\frac{\partial p}{\partial z} + \frac{1}{c_0}\frac{\partial p}{\partial t} = \mathcal{L}p \,, \\ &p(t, z = 0) = f(t) \,. \end{aligned} \tag{15}$$

This PDE is equivalent to the following effective wave equation

$$\begin{aligned} &\frac{\partial^2 p}{\partial z^2} - \frac{1}{c_0^2}\frac{\partial^2 p}{\partial t^2} = \frac{2}{c_0}(\partial_t \mathcal{L})p \,, \\ &p(t, z = 0) = f(t) \,, \quad \partial_z p(t, z = 0) = -\frac{1}{c_0} f'(t) \,. \end{aligned} \tag{16}$$

4.1. *Mixing Random Media*

In this subsection we consider the case of a mixing random medium. We first assume that the typical wavenumber ω/c_0 of the input pulse is such that

$$\frac{|\omega| l_c}{c_0} \ll 1 \,.$$

This condition means that the typical wavelength is longer than l_c and in this case we find that

$$\frac{\gamma_c(\omega)\omega^2}{c_0^2} = \frac{\gamma_c(0)\omega^2}{c_0^2} \,, \tag{17}$$

$$\frac{\gamma_s(\omega)\omega^2}{c_0^2} = 0 \,, \tag{18}$$

which shows that we have an effective second-order diffusion and no effective dispersion.

We next consider the case of a mixing random medium with the linear decay behavior at zero:

$$\phi(z) = \phi(0)\Big(1 - d_{1/2}\frac{|z|}{l_c} + o\Big(\frac{|z|}{l_c}\Big)\Big) \,, \tag{19}$$

with $d_{1/2} \geq 0$. The linear decay of the autocorrelation function is typical of a Markov process, such as the standard Orstein-Uhlenbeck process or the binary (two-component) medium process in the case in which the lengths of the intervals have an exponential distribution. This behavior is in fact very general. For instance the linear decay rate (19) holds for the binary medium process in the case in which the lengths of the intervals have an arbitrary distribution with positive finite expectation. If we assume that the typical wavenumber ω/c_0 of the input pulse is such that

$$\frac{|\omega| l_c}{c_0} \gg 1 \,,$$

which means that the typical wavelength is smaller than l_c, then we have

$$\frac{\gamma_c(\omega)\omega^2}{c_0^2} = \frac{\phi(0) d_{1/2}}{2 l_c} \,, \tag{20}$$

$$\frac{\gamma_s(\omega)\omega^2}{c_0^2} = \frac{\phi(0)\omega}{c_0} \,, \tag{21}$$

which shows that we have an effective constant attenuation and no effective dispersion. In Appendix A we shall discuss the case with an exponentially decorrelating random medium, corresponding to linear decay, without making the high-frequency approximation. We remark that if the medium fluctuations are smooth, corresponding to for instance a Gaussian correlation function, then the wave travels undistorted in this high-frequency regime to leading order. Thus, indeed the medium roughness affects the type of wave deformation one would observe.

4.2. *Random Media with Short-range Correlations*

This is the regime in which the random medium possesses the H-short-range correlation property, $H \in (0, 1/2)$, and the typical wavenumber ω/c_0 of the input pulse is such that

$$\frac{|\omega| l_c}{c_0} \gg 1 \,.$$

This second condition means that the typical wavelength is smaller than l_c and therefore the pulse probes the short-range properties of the medium. In this case we find by using (5), see [14], that

$$\frac{\gamma_c(\omega)\omega^2}{c_0^2} = \phi(0) d_H \frac{\Gamma(1+2H)}{2^{2H}} \sin(H\pi) \frac{1}{l_c} \Big(\frac{|\omega| l_c}{c_0} \Big)^{1-2H} , \tag{22}$$

$$\frac{\gamma_s(\omega)\omega^2}{c_0^2} = \phi(0) \frac{\omega}{c_0} - \phi(0) d_H \frac{\Gamma(1+2H)}{2^{2H}} \cos(H\pi) \Big(\frac{|\omega| l_c}{c_0} \Big)^{-2H} \frac{\omega}{c_0} \,. \tag{23}$$

This result shows that wave propagation in random media with short-range correlations exhibits frequency-dependent attenuation that is characterized by a power law with the exponent $1-2H$ ranging from 0 to 1. This exponent is related to the power decay rate at zero of the autocorrelation function of the medium fluctuations.

In the time domain, we can write

$$\begin{aligned} \mathcal{L}a(\tau) &= \frac{\phi(0)}{8c_0} \frac{\partial a}{\partial \tau} - \frac{\phi(0) d_H}{2^{3+2H} c_0^{1-2H} l_c^{2H}} \int_0^\infty s^{2H} \frac{\partial^2 a}{\partial \tau^2}(\tau - s) ds \\ &= \frac{\phi(0)}{8c_0} \frac{\partial a}{\partial \tau} + \frac{\phi(0) H d_H}{2^{2+2H} c_0^{1-2H} l_c^{2H}} \int_0^\infty \frac{1}{s^{1-2H}} \frac{\partial a}{\partial \tau}(\tau - s) ds \,. \end{aligned} \tag{24}$$

If we go back to the original frame, neglect the random time shift, and substitute the expression (24) of the pseudo-differential operator into (15), we obtain the form of the integro-differential wave equation proposed by Hanyga [16]:

$$\frac{\partial p}{\partial z} + \frac{1}{c_0} \frac{\partial p}{\partial t} = \frac{\phi(0)}{8c_0} \frac{\partial p}{\partial t} + \frac{\phi(0) H d_H}{2^{2+2H} c_0^{1-2H} l_c^{2H}} \int_0^\infty \frac{1}{s^{1-2H}} \frac{\partial p}{\partial t}(t - s) ds \,. \tag{25}$$

If we substitute the expression (24) into (16) we obtain the effective fractional wave equation

$$\frac{\partial^2 p}{\partial z^2} - \frac{1}{c_0^2} \Big(1 + \frac{\phi(0)}{4} \Big) \frac{\partial^2 p}{\partial t^2} = \frac{\phi(0) H d_H}{2^{1+2H} c_0^{2-2H} l_c^{2H}} \int_0^\infty \frac{1}{s^{1-2H}} \frac{\partial^2 p}{\partial t^2}(t - s) ds \,. \tag{26}$$

4.3. *Random Media with Long-range Correlations*

This is the regime in which the random medium has the H-long-range correlation property, $H \in (1/2, 1)$ and the typical wavenumber ω/c_0 of the input pulse is such that

$$\frac{|\omega| l_c}{c_0} \ll 1 \,.$$

This second condition means that the typical wavelength is longer than l_c and therefore the pulse probes the long-range properties of the medium. In this case we find by using (4), see [14], that

$$\frac{\gamma_c(\omega)\omega^2}{c_0^2} = r_H \frac{\Gamma(2H-1)}{2^{2H-2}} \cos\Big((H-\frac{1}{2})\pi\Big) \frac{1}{l_c} \Big(\frac{|\omega| l_c}{c_0}\Big)^{3-2H}, \tag{27}$$

$$\frac{\gamma_s(\omega)\omega^2}{c_0^2} = r_H \frac{\Gamma(2H-1)}{2^{2H-2}} \sin\Big((H-\frac{1}{2})\pi\Big) \Big(\frac{|\omega| l_c}{c_0}\Big)^{2-2H} \frac{\omega}{c_0}. \tag{28}$$

This shows that the wave propagation in random media with long-range correlations exhibits frequency-dependent attenuation that is characterized by a power law with the exponent $3-2H$ ranging from 1 to 2. This exponent is related to the power decay rate at infinity of the autocorrelation function of the medium fluctuations.

In the time domain, we can write

$$\mathcal{L}a(\tau) = \frac{r_H l_c^{2-2H}}{2^{1+2H} c_0^{3-2H}} \int_0^\infty \frac{1}{s^{2-2H}} \frac{\partial^2 a}{\partial \tau^2}(\tau - s) ds\,. \tag{29}$$

If we go back to the original frame and substitute the expression (29) of the pseudo-differential operator into (16) we obtain the effective fractional wave equation

$$\frac{\partial^2 p}{\partial z^2} - \frac{1}{c_0^2}\frac{\partial^2 p}{\partial t^2} = \frac{r_H l_c^{2-2H}}{2^{2H} c_0^{4-2H}} \int_0^\infty \frac{1}{s^{2-2H}} \frac{\partial^3 p}{\partial t^3}(t-s) ds\,. \tag{30}$$

In the next sections we discuss how the precursor emerges as a consequence of the above descriptions.

5. Fractional Precursors

Following [7] we consider in this paper a source function of the form of a step function modulated sine wave

$$f(\tau) = \sin(\omega_c \tau) \mathcal{I}_{\tau>0}\,. \tag{31}$$

The centered transmitted pulse introduced in Section 4 is then given by

$$a(\tau, z) = -\frac{1}{2\pi} \mathrm{Re}\Big[\int_{-\infty}^\infty \frac{1}{\omega - \omega_c} \exp\Big(\frac{z}{c_0}\Phi(\omega,\theta)\Big)\Big], \tag{32}$$

for

$$\Phi(\omega,\theta) = -\frac{\omega^2}{8c_0}\left(\gamma_c(\omega) + i\gamma_s(\omega)\right) - i\omega\theta\,, \qquad \theta = \frac{\tau c_0}{z}\,. \tag{33}$$

The transmitted pulse $a(\tau, z)$ satisfies

$$a(\tau, z) \simeq \sin(\omega_c \tau) \mathcal{I}_{\tau>0}\,, \tag{34}$$

for small propagation distances or in the case with no medium clutter. Our interest is in the case of relatively long propagation distances. The wave is then affected

by the random medium. In fact the wave signal in (34) is exponentially damped. However, as the wave penetrates deep into the medium another signal emerges at the wave front that is not exponentially damped, rather exhibits algebraic decay. This signal is a localized pulse that may serve as a medium probe. Its shape is generic in the sense that it only depends on the medium regime and the associated model parameters discussed above. This means that for long propagation distances we will see a probing pulse whose shape does not depend on the realization, it is *self-averaging* and attains an invariant shape up to scaling. The shape of this function depends on the Hurst parameter in the case of random media with long- and short-range correlations and it spreads out and decays as a fractional power of propagation distance. In analogy with the emergence of precursors in the case of homogeneous dispersive media we refer to the wave that emerges at the front as the *fractional precursor*. We present next the detailed results regarding the random precursors and give the derivation of the results in Section 6.

5.1. *Mixing Media*

We consider the case of a mixing random medium. We discuss in this subsection the low-frequency and the high-frequency regimes, $\omega_c l_c/c_0 \ll 1$ and $\omega_c l_c/c_0 \gg 1$, respectively. For consistency we address in Appendix A the intermediate case $\omega_c l_c/c_0 \sim 1$.

In the low-frequency regime in which the typical wavenumber ω_c/c_0 of the input pulse is such that $\omega_c l_c/c_0 \ll 1$, we have an effective second-order diffusion (17) and no effective dispersion. The phase function appearing in (33) is given by

$$\Phi(\omega,\theta) = -\frac{\gamma_c(0)\omega^2}{8c_0} - i\omega\theta\,. \tag{35}$$

We introduce the parameterization

$$Z = \frac{\gamma_c(0)\omega_c^2}{8c_0^2}z\,, \qquad T = \frac{8c_0}{\gamma_c(0)\omega_c}\theta = \frac{\omega_c\tau}{Z}\,. \tag{36}$$

Note that the first arrival time $\tau(z)$ corresponds to $T = -c_0/(2l_c\omega_c) \ll -1$ in this framework. We find the following characterization for the transmitted pulse:

Proposition 5.1: *In mixing media, if Z is large and T is (at most) of order one, then the transmitted signal has the asymptotic form*

$$a(\tau,z) \overset{Z\gg 1}{\simeq} a_{\rm sp}(T,Z) + a_{\rm p}(T,Z)\,, \tag{37}$$

with

$$a_{\rm sp}(T,Z) = \frac{\exp(-ZT^2/4)}{\sqrt{4\pi Z}}\frac{1}{1+T^2/4}\,,$$
$$a_{\rm p}(T,Z) = \exp(-Z)\sin(ZT)\mathcal{I}_{T>0}\,.$$

The result is based partly on a steepest descent asymptotic approximation (see Subsection 6.1). Here the component $a_{\rm sp}$ is the precursor signal that emerges as the signal penetrates into the medium while $a_{\rm p}$ is the oscillating sine wave component that is exponentially damped with propagation distance. Indeed, in the regime $Z \gg 1$ the signal contribution has a much smaller amplitude than the precursor,

however, we retain it here to articulate how the sine pulse is gradually transformed into the probing precursor.

If we consider a small T, of the order of $Z^{-1/2}$, then we obtain the following corollary:

Corollary 5.2: *In mixing media, if Z is large and $\omega_c\tau$ is smaller than Z, then the transmitted signal has the asymptotic Gaussian form*

$$a(\tau, z) \overset{Z\gg 1}{\simeq} \frac{1}{\sqrt{4\pi Z}} \exp\Big(- \frac{(\omega_c\tau)^2}{4Z}\Big) . \tag{38}$$

In Figure 1 we show the transmitted pulse for two different propagation distances: $Z = 1$ and 20 and with a mixing medium model. The solid line in the figure corresponds to a numerical evaluation of the integral in (32) using the FFT, while the dashed line corresponds to the approximation in (37), and the dashed-dotted line is the Gaussian approximation (38). Initially the pulse is the sine signal in (34). It can be seen that the signal is quickly damped, and as the signal propagates into the medium a coherent pulse emerges at the wave front. Note that with large propagation distance the precursor is indeed to leading order a Gaussian pulse that completely dominates the transmitted sine signal. Regarding the decay of the precursor we have the following result.

Proposition 5.3: *The peak amplitude of the precursor decays as*

$$\max_{\tau} a(\tau, z) \overset{Z\gg 1}{\simeq} \frac{1}{\sqrt{4\pi}} Z^{-1/2} . \tag{39}$$

We remark that the above results are robust in that they hold also for other probing signals than (34), provided that these signals are broadband. Thus, the precursor damping described in Proposition 5.1 is typical for mixing media in the large propagation distance limit.

We comment next on the situation in which the wavenumber ω_c/c_0 is such that $\omega_c l_c/c_0 \gg 1$. We then have an effective constant attenuation and no effective dispersion. The wave propagates therefore without deformation up to an exponential attenuation. In this case we have

$$\Phi(\omega, \theta) = -\frac{\phi(0) c_0 d_{1/2}}{16 l_c} - i\frac{\phi(0)\omega}{8} - i\omega\theta .$$

We introduce in this case the parameterization

$$Z = \frac{\phi(0) d_{1/2}}{16 l_c} z , \tag{40}$$

$$T = \frac{2}{d_{1/2}} \Big(\frac{\omega_c l_c}{c_0}\Big) \Big(1 + \frac{8\theta}{\phi(0)}\Big) = \frac{\omega_c(\tau + \tau_s(z))}{Z} , \tag{41}$$

with $\tau_s(z) = \phi(0)z/(8c_0) = \tau_0(z) - \tau(z)$.

We find then the following characterization for the transmitted pulse:

$$a(\tau, z) = \exp(-Z) \sin(ZT) \mathcal{I}_{T>0} , \tag{42}$$

which only exhibits an exponential decay of the sine wave without deformation. This follows from the fact that attenuation is frequency-independent in this regime.

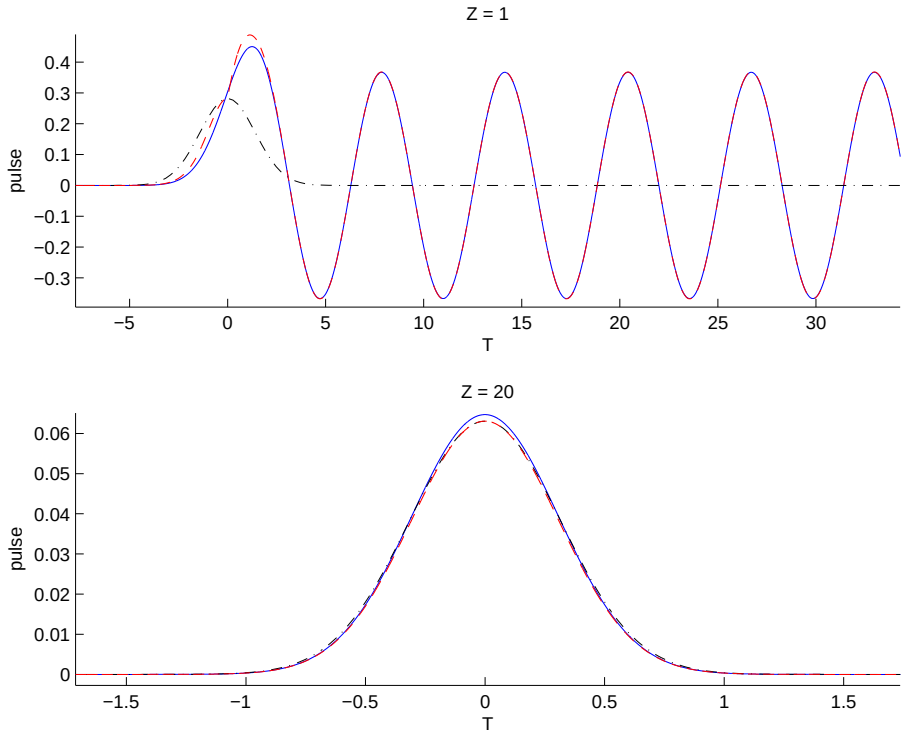

Figure 1. Pulse profile for $Z = 1$ and $Z = 20$ and for a mixing random medium. The pulse is shown as a function of T. The solid line is the exact transmitted pulse (32), the dashed line corresponds to the asymptotic form (37), and the dashed-dotted line is the Gaussian approximation (38). Initially the pulse is the sine signal (34).

We shall find below that the low- and high-frequency limits of the mixing case that we discussed above in Proposition 37 and in Eq. (42) can be obtained from the "low frequency-long range" and the "high frequency-short range" cases discussed in the next two subsections at the limiting value $H = 1/2$ for the Hurst parameter.

5.2. *Random Media with Short-range Correlations*

We consider next the case in which the random medium has the H-short-range correlation property (5) with $H \in (0, 1/2)$. Moreover, we assume the high-frequency regime with a relatively short wavelength so that $\omega_c l_c/c_0 \gg 1$. Now the phase function in (33) takes the form

$$\Phi(\omega,\theta) = -i\omega\frac{\phi(0)}{8} - \frac{\phi(0)d_H\Gamma(1+2H)c_0}{2^{2H+3}l_c}\exp\left(i\pi(H-\frac{1}{2})\right)\left(\frac{\omega l_c}{c_0}\right)^{1-2H} - i\omega\theta\,,$$

which can be derived from (7) and (8), see [14], or explicitly by formula 3.411 in [15].

We introduce a change of coordinates

$$Z = \frac{\phi(0)d_H\Gamma(1+2H)}{2^{2H+3}l_c}\left(\frac{\omega_c l_c}{c_0}\right)^{1-2H} z\,, \tag{43}$$

$$T = \frac{2^{2H}}{d_H\Gamma(1+2H)}\left(\frac{\omega_c l_c}{c_0}\right)^{2H}\left(1+\frac{8\theta}{\phi(0)}\right) = \frac{\omega_c(\tau+\tau_s(z))}{Z}\,, \tag{44}$$

with $\tau_s(z) = \phi(0)z/(8c_0) = \tau_0(z) - \tau(z)$. Note that in view of the discussion

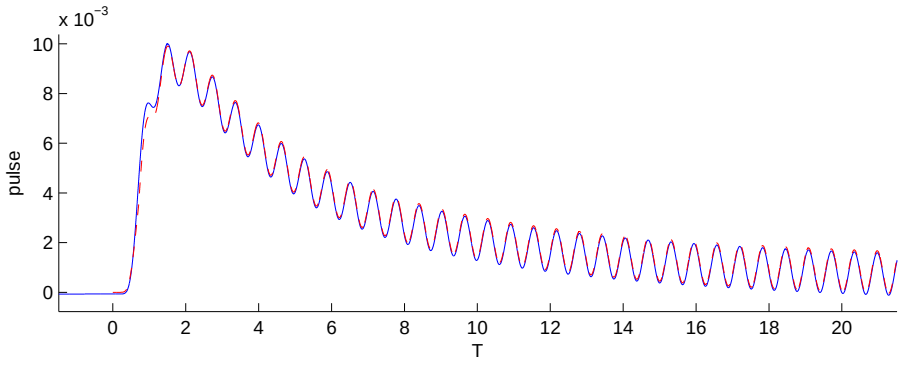

Figure 2. Pulse profile for $Z = 10$ and $H = 1/4$. The pulse is shown as a function of T. The solid line corresponds to the exact transmitted pulse (32) while the dashed line corresponds to the approximation (45).

regarding observation frame in (13) we find that $T = 0$ corresponds to the first arrival time, thus, the transmitted pulse vanishes for $T < 0$.

We show in Subsection 6.2 using a steepest descent approach that the transmitted signal can be approximated as follows.

Proposition 5.4: *In random media with short-range correlations, if Z is large and T is at most of order one, then the transmitted signal has the asymptotic form*

$$a(\tau, z) \overset{Z\gg 1}{\simeq} a_{\rm sp}(T, Z) + a_{\rm p}(T, Z)\,, \tag{45}$$

with

$$a_{\rm sp}(T, Z) = \exp\left(-\frac{\alpha_H^s Z}{T^{\frac{1-2H}{2H}}}\right) \frac{\beta_H^s}{\sqrt{2\pi Z T^{\frac{1+2H}{2H}}}} \frac{T^{\frac{1}{H}}}{T^{\frac{1}{H}} + [(1-2H)]^{\frac{1}{H}}} \mathcal{I}_{T>0}\,,$$
$$a_{\rm p}(T, Z) = \exp\left[-Z\sin(\pi H)\right] \sin\left[Z(T - \cos(\pi H))\right] \mathcal{I}_{T>\cos(\pi H)}\,,$$

where

$$\alpha_H^s = 2H(1-2H)^{\frac{1-2H}{2H}}\,, \qquad \beta_H^s = (2H)^{-\frac{1}{2}}(1-2H)^{\frac{1}{4H}}\,.$$

In the limit $H \uparrow 1/2$ we find:

$$a_{\rm sp}(T, Z) + a_{\rm p}(T, Z) \overset{H\to 1/2}{=} \exp(-Z)\sin(ZT)\mathcal{I}_{T>0}\,.$$

with T, Z defined as in (40), which is the high-frequency regime of the mixing case in (42).

In Figures 2 and 3 we show the transmitted pulse for two different dimensionless propagation distances: $Z = 10, 15$. The solid lines in the figures correspond to a numerical evaluation of the integral in (32) using the FFT, while the dashed lines correspond to the approximation in (45). Again we see how the precursor emerges at the wavefront. We now focus our attention to the shape of the fractional precursor, which is studied in detail in Subsection 6.2.

Proposition 5.5: *In random media with short-range correlations, if Z is large*

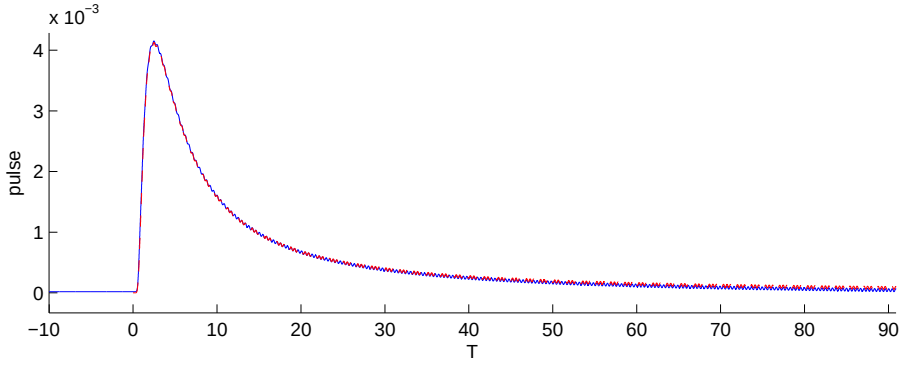

Figure 3. Pulse profile for $Z = 15$ and $H = 1/4$.

then the precursor has the form

$$a(T,Z) \overset{Z\gg 1}{\simeq} Z^{-\frac{1}{1-2H}} A_s\big(TZ^{-\frac{2H}{1-2H}}\big)\,, \tag{46}$$

$$A_s(Y) \;=\; \frac{1}{\pi}\mathrm{Re}\Big[\int_0^\infty \exp\big(-\exp\big(i\pi(H-1/2)\big)u^{1-2H} - iuY\big)du\Big]\,. \tag{47}$$

The precursor shape function A_s has the following properties:
i) For negative Y the value of $A_s(Y)$ is zero.
ii) At $Y = 0$ the function A_s and all its derivatives are zero.
iii) For positive small Y the function A_s can be approximated by

$$A_s(Y) \simeq \frac{\beta_H^s}{\sqrt{2\pi}} Y^{-\frac{1+2H}{4H}} \exp\Big(-\alpha_H^s Y^{-\frac{1-2H}{2H}}\Big)\,. \tag{48}$$

iv) For positive large Y the function A_s can be approximated by

$$A_s(Y) \simeq \frac{1}{\pi}\big[\sin(2H\pi)\Gamma(2-2H)\big]Y^{-(2-2H)}\,. \tag{49}$$

We see from the figures that the multiscale nature of the medium fluctuations changes the nature of the precursor "pulse shaping". First, in the mixing case the decay rate of the peak amplitude is conversely proportional to the square root of the propagation distance. In the short-range correlation case the decay amplitude is different.

Corollary 5.6: *In random media with short-range correlations the peak amplitude of the fractional precursor decays as*

$$\max_T a(T,Z) \overset{Z\gg 1}{\simeq} P_s(H) Z^{-\frac{1}{1-2H}} \tag{50}$$

for $Z \gg 1$, where $P_s(H)$ is a coefficient that depends only on H.

The function $P_s(H)$ is plotted in Figure 4 (left picture) and it can be well approximated (from (48)) by

$$P_s(H) \simeq \frac{1}{\sqrt{2\pi}}\big[2H(1-2H)\big]^{-\frac{1}{1-2H}}\big(H+1/2\big)^{\frac{H+1/2}{1-2H}} \exp\Big(-\frac{H+1/2}{1-2H}\Big)\,. \tag{51}$$

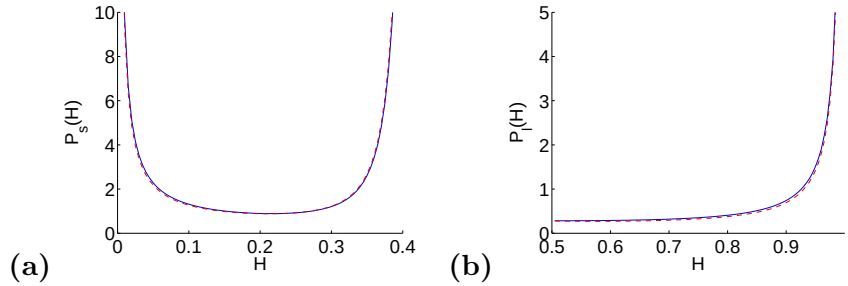

Figure 4. Coefficients $P_s(H)$ (picture a) and $P_l(H)$ (picture b). The solid lines are the exact values. In picture a, the dashed line is the approximation (51). In picture b, the dashed line is the approximation (62).

The power law decay $Z^{-\frac{1}{1-2H}}$ with the decay rate $\frac{1}{1-2H} \in (1,\infty)$ is characteristic of random media with short-range correlations. It is different from the power decay with decay rate $Z^{-1/2}$ observed in mixing media.

In the mixing case discussed above the asymptotic shape is Gaussian. In particular the tail of the precursor decays super-exponentially in time as (38). In the case with a random medium with short-range correlations the asymptotic shape is skewed with a power law decay for large times that depends on the Hurst parameter. In fact the right tail of the fractional precursor has a power law decay in time reflecting the short-range correlation properties of the random medium. The power law can be identified in the regime of large times and we next quote the result that characterizes this aspect of the pulse shaping that carries in it the signature of the medium class.

Corollary 5.7: *If* $T^{\frac{1-2H}{2H}} \gg Z \gg 1$ *then we have*

$$a(T,Z) \simeq \frac{\sin(2H\pi)\Gamma(2-2H)}{\pi} Z^{-(1-2H)} T^{-(2-2H)}\,. \tag{52}$$

Since $T = \omega_c(\tau + \tau_s(z))/Z$, this statement is equivalent to the following one: If $[\omega_c(\tau+\tau_s(z))]^{1-2H} \gg Z \gg 1$ then we have

$$a(\tau,z) \simeq \frac{\sin(2H\pi)\Gamma(2-2H)}{\pi} \frac{Z}{[\omega_c(\tau+\tau_s(z))]^{2-2H}}\,. \tag{53}$$

See Subsection 6.2 for the derivation. We illustrate the tail behavior and the good match with the theoretical predictions in Figures 5 and 6 for the Hurst parameter being respectively $H = 0.1$ and $H = 0.3$.

5.3. *Random Media with Long-range Correlations*

We consider the case in which the random medium has the long-range correlation property (4) with $H \in (1/2, 1)$ and the low-frequency regime $\omega_c \ll c_0/l_c$. Now the phase function in (33) takes the form

$$\Phi(\omega,\theta) = -\frac{c_0 r_H \Gamma(2H-1)}{2^{2H+1} l_c} \exp\left(i\pi(H-\frac{1}{2})\right)\left(\frac{\omega l_c}{c_0}\right)^{3-2H} - i\omega\theta\,.$$

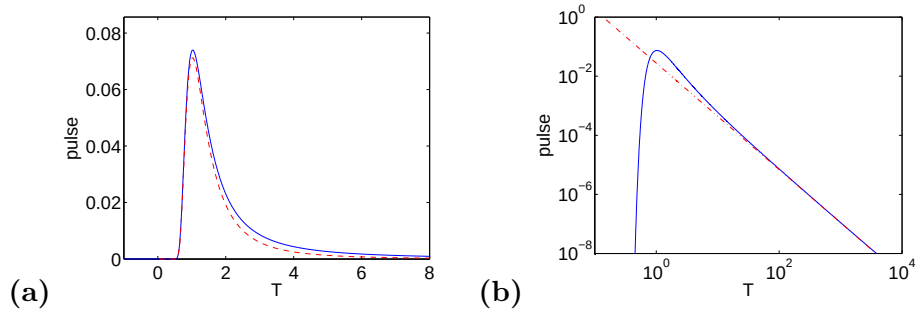

Figure 5. Precursor profile for $H = 0.1$, $Z = 10$, in linear (picture a) and logarithmic (picture b) scales, as a function of T. The solid line is the theoretical expression (46-47) of the precursor. The dashed line (in picture a) corresponds to the approximate expression (48) substituted into (46), which gives a good approximation of the central form of the precursor. The dot-dashed line (in picture b) is the asymptotic formula (52), which gives a good approximation of the positive tail of the precursor.

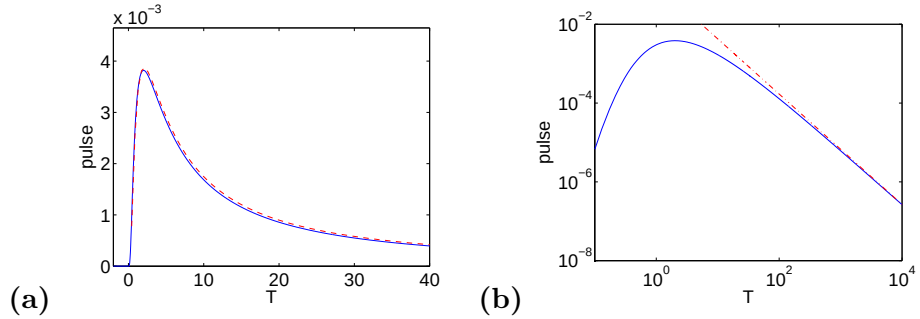

Figure 6. Same as in Figure 5, but for $H = 0.3$, $Z = 10$.

We introduce the change of coordinates

$$Z = \frac{r_H \Gamma(2H-1)}{2^{2H+1} l_c} \left(\frac{\omega_c l_c}{c_0}\right)^{3-2H} z\,, \tag{54}$$

$$T = \frac{2^{2H+1}}{r_H \Gamma(2H-1)} \left(\frac{\omega_c l_c}{c_0}\right)^{2H-2} \theta = \frac{\omega_c \tau}{Z}\,. \tag{55}$$

Using a steepest descent approach, we find the following result in Subsection 6.3, which shows that the step function modulated sine wave is exponentially damped and that a precursor appears at the front.

Proposition 5.8: *In random media with long-range correlations, if Z is large and T is of order one and negative, then the transmitted signal has the asymptotic form*

$$a(\tau, z) \overset{Z \gg 1}{\simeq} a_{\rm sp}(T, Z) + a_{\rm p}(T, Z)\,, \tag{56}$$

with

$$a_{\rm sp}(T, Z) = \exp\left(-\alpha_H^l Z |T|^{\frac{3-2H}{2-2H}}\right) \frac{\beta_H^l |T|^{\frac{2H-1}{4-4H}}}{\sqrt{2\pi Z}} \frac{1}{1 + \left(\frac{|T|}{3-2H}\right)^{\frac{1}{1-H}}}\,,$$

$$a_{\rm p}(T, Z) = \exp\left[-Z \sin(\pi H)\right] \sin\left[Z(T - \cos(\pi H))\right] \mathcal{I}_{T > \cos(\pi H)}\,,$$

where

$$\alpha_H^l = (2-2H)(3-2H)^{-\frac{3-2H}{2-2H}}\,, \qquad \beta_H^l = (2-2H)^{-\frac{1}{2}}(3-2H)^{-\frac{1}{4-4H}}\,.$$

We remark that as $H \downarrow 1/2$ the limiting pulse shape approaches the Gaussian shape and is centered around $T = 0$. One can check explicitly that this limit gives the signal in (37) of the low-frequency regime in the mixing case.

For $T \geq 0$ the direct evaluation via the steepest descent method at the stationary point does not give the leading contribution, however, we shall get the precursor behavior and its power law decay via an integral expression as we discuss next. We remark that the approximation $a_{\rm p}$ for the damped sine wave component holds also for $T > 0$.

In Figures 7 and 8 we show the transmitted pulse for two different propagation distances: $Z = 4,400$ and $H = 0.9$. The solid line in the figure corresponds to a numerical evaluation of the integral in (32) using the FFT, while the dashed line corresponds to the asymptotic approximation in (56).

The pulse shape of the precursor for arbitrary value of T is obtained in Subsection 6.3 and we give it in the following proposition.

Proposition 5.9: *In random media with long-range correlations, if Z is large then the precursor has the form*

$$a(T,Z) \overset{Z\gg 1}{\simeq} Z^{-\frac{1}{3-2H}} A_l\big(TZ^{\frac{2-2H}{3-2H}}\big)\,, \tag{57}$$

$$A_l(Y) \;=\; \frac{1}{\pi}\mathrm{Re}\Big[\int_0^\infty \exp\big(-\exp\big(i\pi(H-1/2)\big)u^{3-2H} - iuY\big)du\Big]\,. \tag{58}$$

The precursor shape function A_l has the following properties:
i) At $Y = 0$ the function A_l and its derivatives are given by:

$$\frac{\partial^k A_l}{\partial Y^k}(0) = \frac{1}{(3-2H)\pi}\cos\Big(\frac{\pi}{2}\frac{1-2(H+k)}{3-2H}\Big)\Gamma\Big(\frac{1+k}{3-2H}\Big)\,.$$

ii) For negative large Y the function A_l can be approximated by

$$A_l(Y) \simeq \frac{\beta_H^l}{\sqrt{2\pi}}|Y|^{\frac{2H-1}{4-4H}}\exp\Big(-\alpha_H^l|Y|^{\frac{3-2H}{2-2H}}\Big)\,. \tag{59}$$

iii) For positive large Y the function A_l can be approximated by

$$A_l(Y) \simeq \frac{1}{\pi}\big[-\sin(2H\pi)\Gamma(4-2H)\big]Y^{-(4-2H)}\,. \tag{60}$$

We see from Figures 9 and 10 that the long-range correlations in the medium again change the precursor qualitatively. First, the peak amplitude of the precursor has a anomalous power decay different from the usual decay rate $Z^{-1/2}$ observed in mixing media.

Corollary 5.10: *In random media with long-range correlations the peak amplitude of the fractional precursor decays as*

$$\max_T a(T,Z) \overset{Z\gg 1}{\simeq} P_l(H)Z^{-\frac{1}{3-2H}}\,, \tag{61}$$

where $P_l(H)$ is a coefficient that depends only on H.

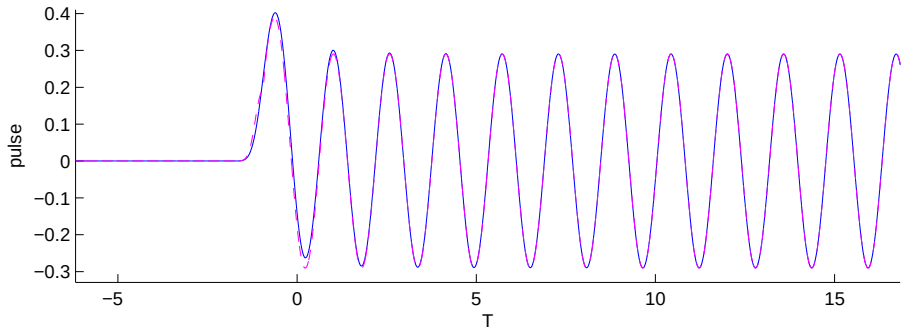

Figure 7. Pulse profile for $Z = 4$ and $H = 0.9$. The pulse is shown as a function of T. The solid line is the exact transmitted pulse (32) while the dashed line corresponds to the approximation (56).

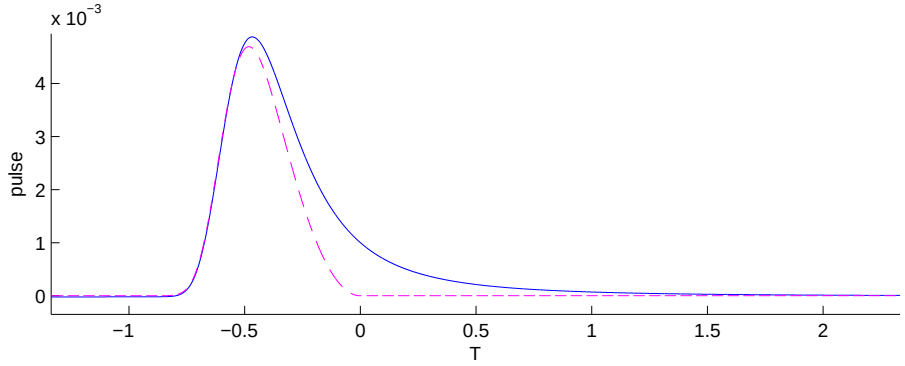

Figure 8. As Figure 7, but with $Z = 400$.

The function $P_l(H)$ is plotted in Figure 4 (right picture) and it can be well approximated (from (59)) by

$$P_l(H) \simeq \frac{1}{\sqrt{2\pi}}\big[(2-2H)(3-2H)\big]^{-\frac{1}{3-2H}}\big(H-1/2\big)^{\frac{H-1/2}{3-2H}}\exp\Big(-\frac{H-1/2}{3-2H}\Big)\,. \quad (62)$$

The power law decay $Z^{-\frac{1}{3-2H}}$ with the decay rate $\frac{1}{3-2H} \in (1/2, 1)$ is characteristic of random media with long-range correlations. It is different from the power decay with decay rate $1/2$ observed in mixing media.

Second, the pulse develops an anomalous power law decay for large times. We have the following proposition characterizing this effect.

Corollary 5.11: *If $T \gg Z^{\frac{2H-2}{3-2H}}$ and $Z \gg 1$, then we have*

$$a(T,Z) \simeq \frac{-\sin(2H\pi)\Gamma(4-2H)}{\pi} Z^{-(3-2H)} T^{-(4-2H)}\,. \quad (63)$$

Since $T = \omega_c\tau/Z$, this statement is equivalent to the following one: If $(\omega_c\tau)^{3-2H} \gg Z \gg 1$ then we have

$$a(\tau,z) \simeq \frac{-\sin(2H\pi)\Gamma(4-2H)}{\pi} \frac{Z}{(\omega_c\tau)^{4-2H}}\,. \quad (64)$$

We show in Figures 9 and 10 the excellent match of the theoretical power law prediction with the explicit calculation of the tail via computation of the integral in (32).

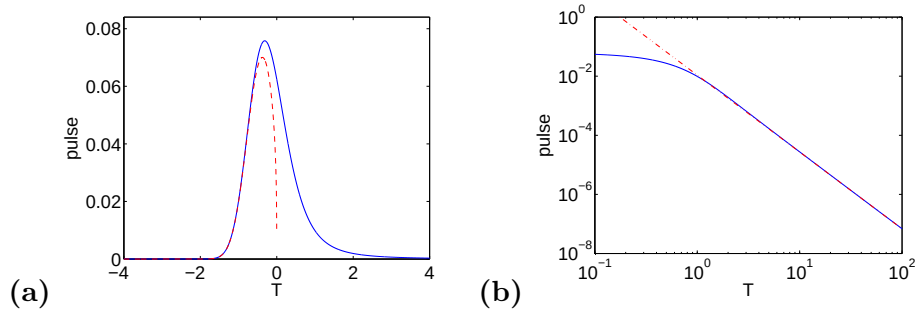

Figure 9. Precursor profile for $H = 0.7$, $Z = 10$, in linear (picture a) and logarithmic (picture b) scales as a function of T. The solid line is the theoretical expression (57-58) of the precursor. The dashed line (in picture a) corresponds to the approximate expression (59) substituted into (57), which gives a good approximation of the precursor at negative times. The dot-dashed line (in picture b) is the asymptotic formula (63), which gives a good approximation of the positive tail of the precursor.

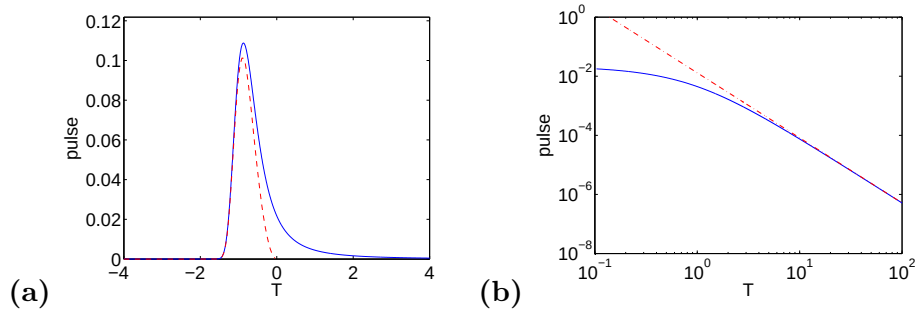

Figure 10. Same as in Figure 9, but for $H = 0.9$, $Z = 10$.

6. Derivation of the Main Results

6.1. *Mixing Media*

We consider the medium regime discussed in Subsection 5.1 and derive the results presented there. We use the parameterization in (36), moreover, denote $\Omega = \omega/\omega_c$. The expression (32) for the transmitted pulse becomes

$$a(\tau, z) = -\frac{1}{2\pi}\mathrm{Re}\Big[\int_{-\infty}^{\infty} \frac{1}{\Omega - 1} \exp\big(Z\Phi_m(\Omega, T)\big) d\Omega\Big], \tag{65}$$

with the phase function

$$\Phi_m(\Omega, T) = -\Omega^2 - i\Omega T\,.$$

We plot the real and imaginary parts of Φ_m in Figure 11 for $T = 1$ and as a function of complex frequency Ω. We have a unique saddle point in the complex plane given by $\Omega^* = -iT/2$. The saddle point is shown by the diamond in the figure, the pole by the cross. The steepest descent path is in this case parallel to the abscissa and can be joined with the original integration path for some large absolute value for the real part of Ω. We have also a contribution in terms of the residue at the pole at ω_c, that is $\Omega = 1$, giving rise to the "signal" component a_{p}. Applying now the method of steepest descent and computing the signal contribution via the associated residue we find that we can approximate the integral (65) as in (37).

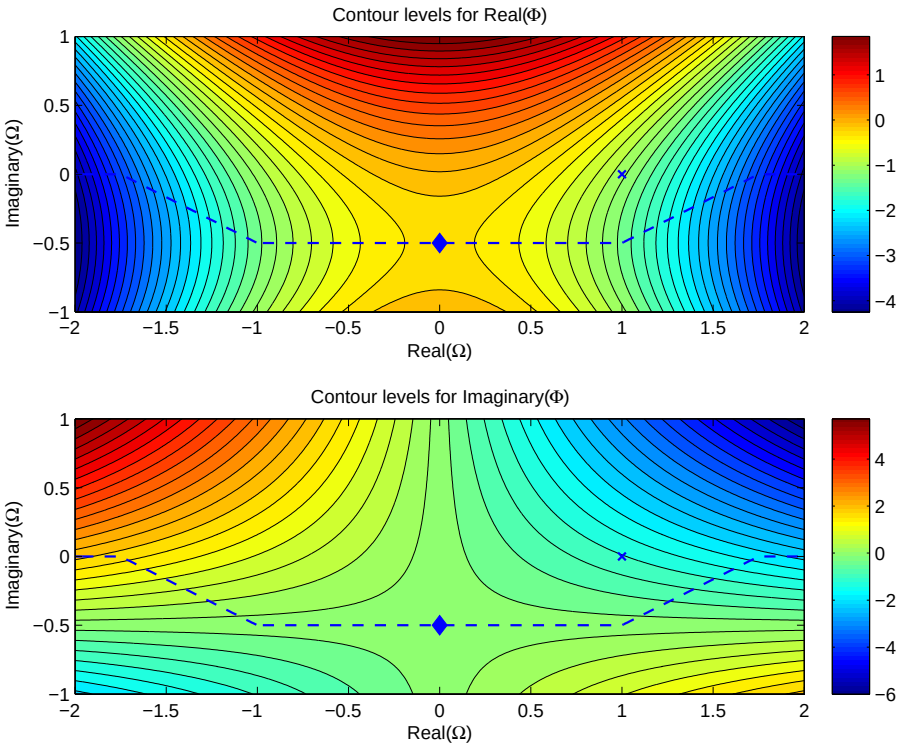

Figure 11. Contour plot of Real(Φ) and Imag(Φ) for $T = 1$. Case of a random mixing medium. The diamond corresponds to the saddle point while the cross corresponds to the pole and the dashed line is the integration path.

6.2. *Random Media with Short-range Correlations*

We consider the medium regime discussed in Subsection 5.2 and derive the results discussed there with $\omega_c \gg c_0/l_c$. We use notations as in the previous subsection. Here $T = 0$ corresponds to the first arrival time, thus, the transmitted pulse vanishes for $T < 0$. The expression (32) for the transmitted pulse becomes

$$a(\tau, z) = -\frac{1}{2\pi}\mathrm{Re}\Big[\int_{-\infty}^{\infty} \frac{1}{\Omega - 1} \exp\big(Z\Phi_s(\Omega, T)\big) d\Omega\Big], \tag{66}$$

with the phase function now taking the form

$$\Phi_s(\Omega, T) = -\exp\big(i\pi(H - 1/2)\big)\,\Omega^{1-2H} - i\Omega T\,.$$

We plot the real and imaginary parts of Φ_s in Figure 12 for $H = 0.3$ and $T = 0.5$. For $T > 0$ the saddle point is given by

$$\Omega^* = i\Big(\frac{1-2H}{T}\Big)^{1/(2H)}.$$

Thus, we have a unique saddle point in the upper complex half-plane. The saddle point is shown by the diamond in the figure, the pole by the cross and the steepest descent path from the top saddle point joining the original integration path by the dashed line. Applying again the method of steepest descent and computing the contribution of the residue associated with the signal pole we arrive at the approximation in (45).

We next derive the results in Proposition 5.5 and Corollaries 5.6-5.7. We give the

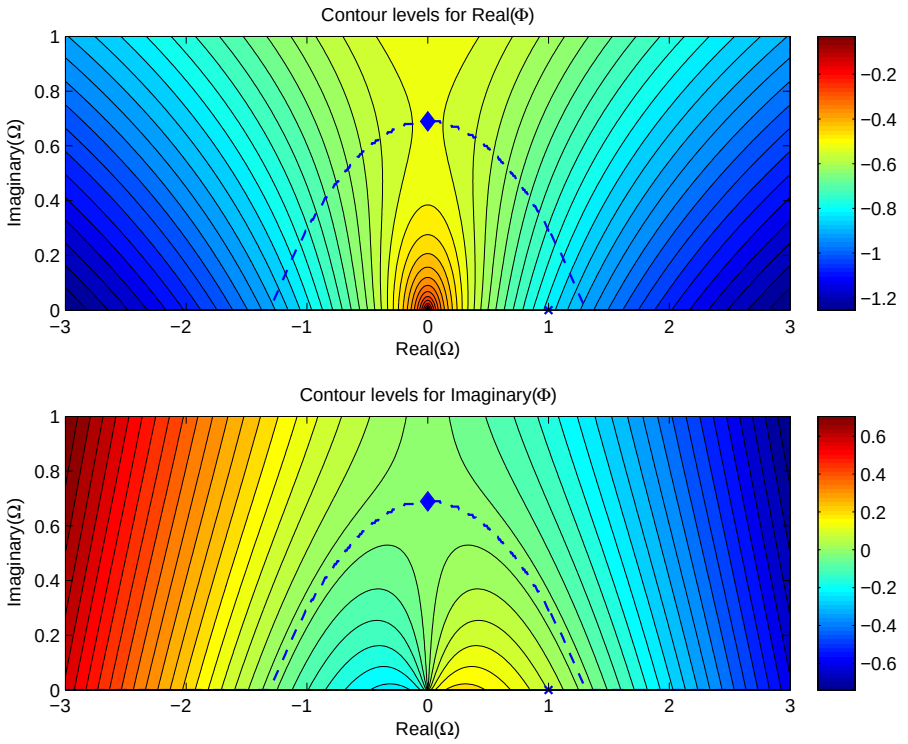

Figure 12. Contour plot of Real(Φ) and Imag(Φ) for $H = 0.3$ and $T = 0.5$.

main steps of the proof while the technical details are given in Appendices B and C. The pulse profile is given by (66). The following lemma shows that the pole at $\Omega = 1$ is asymptotically negligible in that it gives a contribution to the transmitted pulse profile that is small in Z (i.e. smaller than the precursor amplitude). This expresses the fact that the step function modulated sine wave signal is damped and becomes negligible compared to the precursor signal (67) that appears at the front.

Lemma 6.1: *There exists a constant K_H such that:*

$$\Big|a(T,Z) - \frac{1}{\pi}\mathrm{Re}\Big[\int_0^\infty \exp\big(Z\Phi_s(\Omega,T)\big)d\Omega\Big]\Big| \le K_H Z^{-\frac{2}{1-2H}}\,. \tag{67}$$

Proof: See Appendix B. □

Next, using the change of variable $\Omega = uZ^{-1/(1-2H)}$ in the expression of the precursor in (67) we obtain the statement of Proposition 5.5. The function A_s defined by (47) is the dimensionless pulse profile of the precursor in media with short-range correlations. We have in particular

$$\max_T a(T,Z) = \big[\max_Y A_s(Y)\big] Z^{-\frac{1}{1-2H}}\,,$$

which gives Corollary 5.6. The analysis of the large-Y behavior of $A_s(Y)$ and the result (49) is based on a variant of the Abelian theorem 7(i) in [24] which is detailed in Appendix C. By substituting (49) into the expression (47) of the precursor we obtain the result of Corollary 5.7. Note that the two hypotheses of Corollary 5.7 are equivalent to $T^{\frac{1-2H}{2H}} \gg Z \gg 1$ or $[\omega_c(\tau+\tau_s)]^{1-2H} \gg Z \gg 1$ (since $T = [\omega_c(\tau+\tau_s)]/Z$). In the (τ, Z) variables we obtain (53). We remark that the

error bound in Lemma 6.1 gives a corresponding limit on the range of T in (52):

$$T \ll Z^{\frac{1+4H-4H^2}{(1-2H)(2-2H)}} ,$$

to assure that the approximation dominates the error bound in (67). Finally, note that the result (48) can be obtained via a steepest descent approximation.

6.3. *Random Media with Long-range Correlations*

We consider the medium regime discussed in Subsection 5.3 and derive the results discussed there with $\omega_c \ll c_0/l_c$. We use here the parameterization in (54) and the expression (32) for the transmitted pulse becomes

$$a(T,Z) = -\frac{1}{2\pi}\mathrm{Re}\Big[\int \frac{1}{\Omega - 1}\exp\big(Z\Phi_l(\Omega,T)\big)d\Omega\Big] , \tag{68}$$

with the phase function now taking the form

$$\Phi_l(\Omega,T) = -\exp\big(i\pi(H-1/2)\big)\,\Omega^{3-2H} - i\Omega T\,.$$

We plot the real and imaginary parts of Φ_l in Figure 13 for $H = 0.75$ and $T = -2$. The saddle point for $T < 0$ is given by

$$\Omega^* = i\Big(\frac{|T|}{3-2H}\Big)^{1/(2-2H)} .$$

Thus, we have a single saddle point in the upper complex half-plane. The saddle point is shown by the diamond in the figure, the pole by the cross and the steepest descent path from the saddle point joining the original integration path by the dashed line. Applying again the method of steepest descent and evaluating the pole contribution we find that we can approximate as in (56).

We now give the main steps of the proof of Proposition 5.9 and Corollaries 5.10-5.11 of Subsection 5.3. The details are given in the appendices. The pulse profile is given by (68). As in the case of media with short-range correlations the first step shows that the step function modulated sine wave signal is exponentially damped and becomes negligible compared to the precursor signal (69) that appears at the front.

Lemma 6.2: *There exists a constant K_H such that:*

$$\Big|a(T,Z) - \frac{1}{\pi}\mathrm{Re}\Big[\int_0^\infty \exp\big(Z\Phi_l(\Omega,T)\big)d\Omega\Big]\Big| \le K_H Z^{-\frac{2}{3-2H}} . \tag{69}$$

Proof: The proof follows the same line as in the case of a medium with short-range correlations. □

Using the change of variable $\Omega = uZ^{-1/(3-2H)}$ in the expression of the precursor in (69) we find the statement of Proposition 5.9. The function A_l defined by (58) is the dimensionless pulse profile of the precursor in media with long-range correlations. We have in particular

$$\max_T a(T,Z) = \big[\max_Y A_l(Y)\big] Z^{-\frac{1}{3-2H}} ,$$

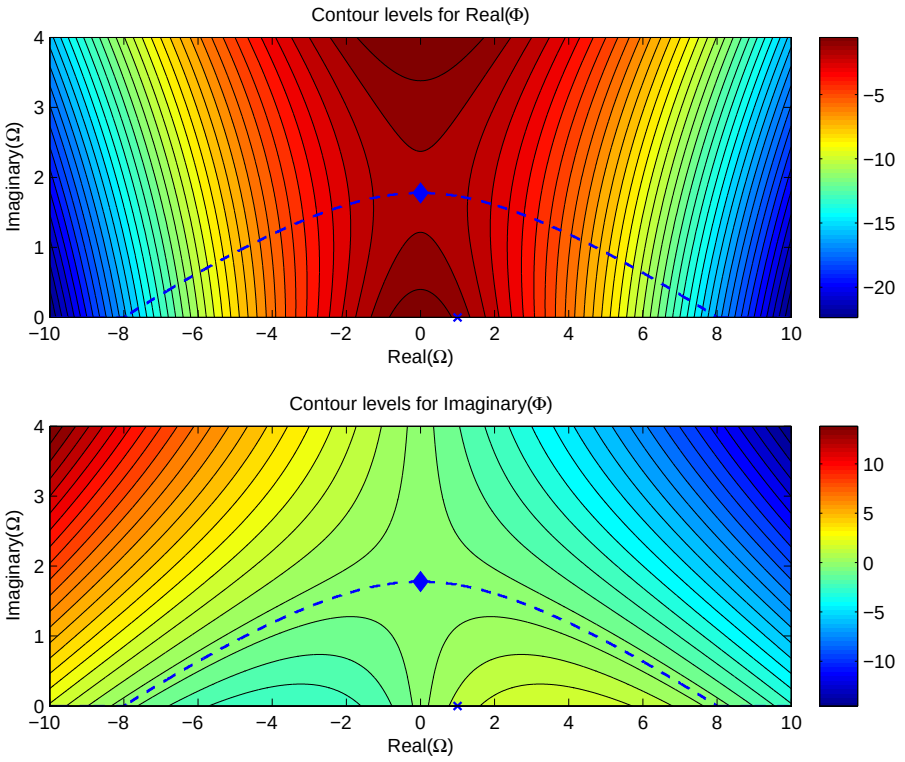

Figure 13. Contour plot of Real(Φ) and Imag(Φ) for $T = -2, H = 0.75$.

which gives Corollary 5.10. The large-Y behavior of $A_l(Y)$ follows from an Abelian theorem as explained in Appendix C. By substituting (60) into the expression (58) of the precursor we obtain the result of Corollary 5.11. Note that the two hypotheses of Corollary 5.11 are equivalent to $T^{-\frac{3-2H}{2-2H}} \gg Z \gg 1$ or $(\omega_c\tau)^{3-2H} \gg Z \gg 1$. In the (τ, Z) variables we then obtain (64).

7. Conclusion

We have considered wave propagation in one-dimensional random media. The probing signal experiences a self-averaging deformation by interacting with the medium. This can be seen as a "law of large number result" in that many double scattering events, backward and then forward scattering of wave energy, adds up with propagation distance to give the deterministic deformation. The character of the deformation depends on the medium class and long- or short-range correlations in the medium in particular lead to an anomalous and skewed power law shape for the pulse. What is not so intuitive is that this phenomenon takes place even when the source signal is not pulse like, but for instance a stepped sine signal as we have considered in this paper constituting the broadband source. Then at the front of the sine wave the scattering builds a coherent wave pulse which travels much deeper than the sine signal itself, it experiences an algebraic decay with propagation distance rather than exponential. An intuitive argument for this situation is that at the front of the sine the broad band nature of the signal builds the precursor, while far behind the front the stepped sine source has a monochromatic nature. In Figure 14 we summarize the picture: the solid line plots the exponent of the frequency-dependent power law attenuation as described in Section 4, which corresponds to the order of the time derivative in the fractional wave equation; the

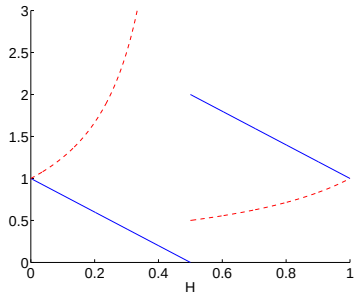

Figure 14. The fractional time derivative order in the fractional wave equation (solid line) and the damping power for the precursor (dashed line) as functions of Hurst index H.

dashed line shows the damping power of the precursor associated with the fractional wave equation. The fractional precursor is damped as the reciprocal of the propagation distance to the damping power. The antipersistent case $H \in (0, 1/2)$ corresponds to relative high-frequency waves and the medium roughness being the principal effect, while the persistent case corresponds to $H \in (1/2, 1)$ and the medium long-range correlations being the principal effect in terms of generation and damping of the precursor.

We have here presented a first analysis of the "fractional precursor" phenomenon. Many important questions remain. For instance the robustness of the result with respect to the medium model, in particular with respect to the one-dimensional assumption that we have made here and also with respect to the scaling assumptions in the underlying theory. Moreover, how this phenomenon can be relevant in applications analogous to those where the classical precursors of homogeneous dispersive media have plaid a role.

8. Acknowledgement

We are grateful to Dr. Arje Nachman for suggesting the problem we have considered in this paper and pointing out to us the prospect of fractional precursors.

Appendix A. Mixing and Exponentially Decorrelating Media

We consider here the case with the correlation function for the medium fluctuations being

$$\phi(z) = \mathbb{E}[\nu(y)\nu(y+z)] = \phi(0)\exp(-|z|/l_c)\,. \tag{A1}$$

As remarked above the behavior at the origin of this correlation function is rather general. We present it here to illustrate the intermediate case with $(c_0/l_c)/\omega_c = \mathcal{O}(1)$. We remark moreover that this model has common features with the Lorentz dielectric model of the classical situation analyzed for precursors in homogeneous dispersive media [7]. The phase function in (33) is now

$$\Phi(\omega,\theta) = -i\left(\frac{\phi(0)\omega^2}{8(\omega + ic_0/(2l_c))} + \omega\theta\right)\,.$$

We introduce the parameterization

$$Z = \frac{\phi(0)\omega_c}{8c_0} z\,, \qquad T = 1 + \frac{8\theta}{\phi(0)} = 1 + \frac{\omega_c \tau}{Z}\,, \tag{A2}$$

and the mixing parameter

$$\delta_m = \frac{c_0}{2\omega_c l_c}\,.$$

The limit case $\delta_m \to \infty$, resp. $\delta_m \to 0$, corresponds to the low-frequency, resp. high-frequency, regime. Note also that in view of the discussion regarding travel time presented in Section 4 we find that $T = 0$ corresponds to the first arrival time, thus, the transmitted pulse vanishes for $T < 0$. We then find the following characterization for the transmitted pulse:

Proposition A.1: *Under the model (A1), if Z is large and T is of order one, then the transmitted signal has the asymptotic form*

$$a(\tau, z) \overset{Z \gg 1}{\simeq} a_{\rm sp}(T, Z) + a_{\rm p}(T, Z)\,, \tag{A3}$$

with

$$a_{\rm sp}(T, Z) = \frac{\exp(-Z\delta_m(1-\sqrt{T})^2)}{\sqrt{4\pi Z T^{3/2}/\delta_m}} \frac{T}{T + \delta_m^2(1-\sqrt{T})^2} \mathcal{I}_{T>0}\,,$$

$$a_{\rm p}(T, Z) = \exp\left(-\frac{Z\delta_m}{1+\delta_m^2}\right) \sin\left(Z\Big(T - \frac{\delta_m^2}{1+\delta_m^2}\Big)\right) \mathcal{I}_{T>\delta_m^2/(1+\delta_m^2)}\,.$$

The result follows again by a steepest descent argument. Here the component $a_{\rm sp}$ is the precursor signal that emerges as the signal penetrates into the medium while $a_{\rm p}(T, Z)$ is the oscillating "signal" component that is exponentially damped with the propagation distance.

If $\delta_m \to \infty$, then we recover the statement of Proposition 5.1 in the low-frequency regime, after the change of variables $Z \to \delta_m Z$ and $T \to 1 + T/\delta_m$. Similarly, if $\delta_m \to 0$ then we recover the asymptotic approximation (42) valid in the high-frequency regime, after the change of variables $Z \to Z/\delta_m$ and $T \to \delta_m T$. If δ_m is of order one and Z is large, then the following corollaries show that the peak amplitude of the precursor has a power law decay and that the shape of the precursor is Gaussian as in the low-frequency regime $\delta_m \to \infty$.

Corollary A.2: *The peak amplitude of the precursor decays as*

$$\max_\tau a(\tau, z) \overset{Z \gg 1}{\simeq} \frac{1}{\sqrt{4\pi/\delta_m}} Z^{-1/2}\,. \tag{A4}$$

Corollary A.3: *If Z is large and $\omega_c\tau$ is smaller than Z, then we have*

$$a(\tau, z) \simeq \frac{1}{\sqrt{4\pi Z/\delta_m}} \exp\Big(-\frac{\delta_m(\omega_c\tau)^2}{4Z}\Big)\,. \tag{A5}$$

In Figures A1, A2, A3 and A4 we show the transmitted pulse for four different propagation distances: $Z = 2, 10, 20, 100$, moreover, with the mixing parameter $\delta_m = 1$. The solid lines in the figures correspond to numerical evaluations of the

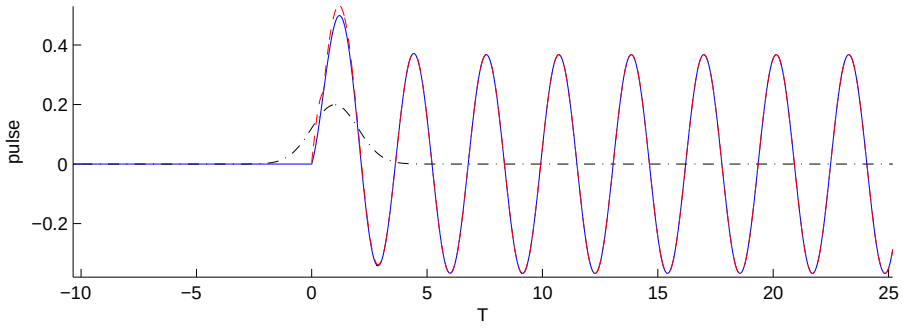

Figure A1. Pulse profile for $Z = 2$ and for a mixing random medium with $\delta_m = 1$. The pulse is shown as a function of T. The solid line is the exact transmitted pulse (32), the dashed line corresponds to the approximation (A3), and the dashed-dotted line is the Gaussian approximation (A5).

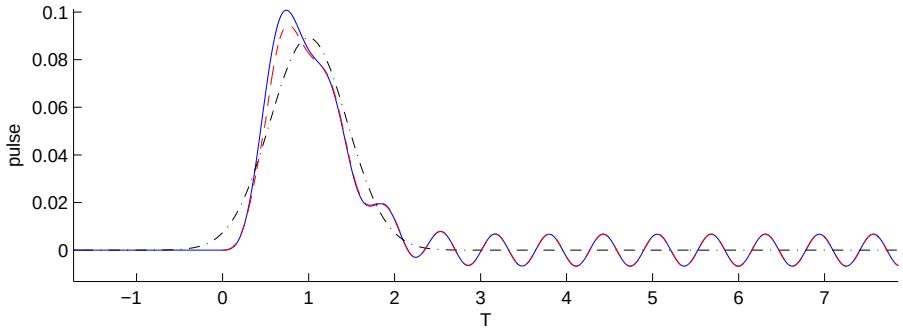

Figure A2. Pulse profile for $Z = 10$.

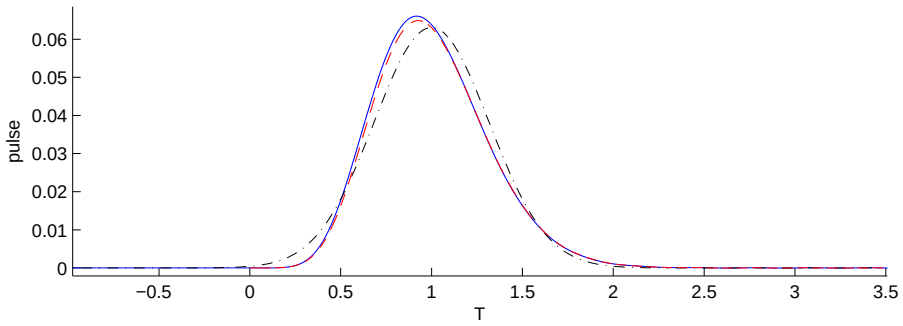

Figure A3. Pulse profile for $Z = 20$.

integral in (32) using the FFT, while the dashed lines correspond to the approximation (A3) and the dashed-dotted lines correspond to the Gaussian approximation (A5) with $\omega_c\tau = Z(T-1)$ (according to (A2)) .

Appendix B. Proof of Lemma 6.1

We give here the proof of Lemma 6.1 in the short-range case $H \in (0, 1/2)$. The proof of Lemma 6.2 in the long-range case $H \in (1/2, 1)$ can be addressed in the same way. We first show the following lemma.

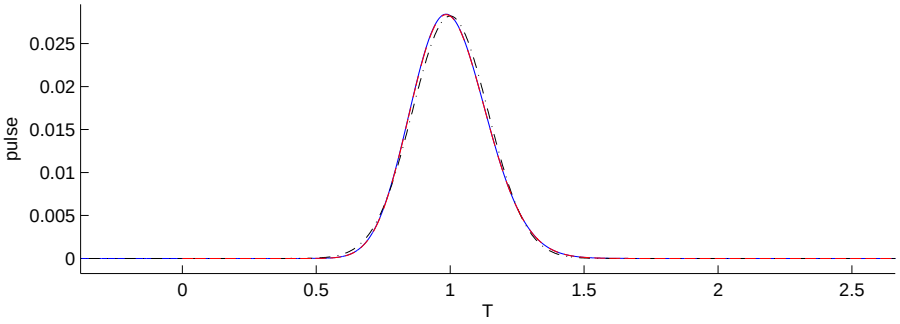

Figure A4. Pulse profile for $Z = 100$.

Lemma B.1: *The integrals*

$$\int_{|\Omega|>1/2} \frac{1}{1-\Omega} \exp\big(Z\Phi_s(\Omega,T)\big)d\Omega \quad \textit{and} \quad \int_{|\Omega|>1/2} \exp\big(Z\Phi_s(\Omega,T)\big)d\Omega$$

are exponentially decaying in Z.

Proof: We write

$$Z\Phi_s(\Omega,T) = -Z\psi(\Omega) - iZ\Omega T, \qquad \psi(\Omega) = \psi_r(\Omega) + i\psi_i(\Omega),$$

with $\psi_r(\Omega) = \cos(\pi(H-1/2))|\Omega|^{1-2H}$ and $\psi_i(\Omega) = \sin(\pi(H-1/2))|\Omega|^{-2H}\Omega$. We first look at the integral from $1/2$ to $3/2$:

$$\begin{aligned}\mathrm{Re}\Big[\int_{\frac12}^{\frac32} \frac{1}{\Omega-1} e^{Z\Phi(\Omega,T)}d\Omega\Big] &= \mathrm{Re}\Big[\int_{\frac12}^{\frac32} \frac{1}{\Omega-1} e^{-Z\psi(1)}e^{-i\Omega T}d\Omega\Big] \\ &\quad + \mathrm{Re}\Big[\int_{\frac12}^{\frac32} \frac{1}{\Omega-1}\big(e^{-Z\psi(\Omega)} - e^{-Z\psi(1)}\big)e^{-i\Omega T}d\Omega\Big].\end{aligned}$$

Using the fact that $[1/2, 3/2]$ is an interval symmetric with respect to 1 we find

$$\begin{aligned}\Big|\mathrm{Re}\Big[\int_{\frac12}^{\frac32} \frac{1}{\Omega-1} e^{-Z\psi(1)}e^{-i\Omega T}d\Omega\Big]\Big| &= \Big|\mathrm{Re}\Big[e^{-Z\psi(1)}e^{-iT}\int_{-\frac12}^{\frac12} \frac{1}{\Omega} e^{-i\Omega T}d\Omega\Big]\Big| \\ &= \Big|\mathrm{Re}\Big[-ie^{-Z\psi(1)}e^{-iT}\int_{-T/2}^{T/2} \frac{\sin(u)}{u}du\Big]\Big| \\ &\le K_1 e^{-Z\psi_r(1)}, \qquad K_1 = 2\sup_{U>0}\Big|\int_0^U \frac{\sin(u)}{u}du\Big|,\end{aligned}$$

Morevover

$$\begin{aligned}\Big|\mathrm{Re}\Big[\int_{\frac12}^{\frac32} \frac{1}{\Omega-1}\big(e^{-Z\psi(\Omega)} - e^{-Z\psi(1)}\big)e^{-i\Omega T}d\Omega\Big]\Big| &\le \int_{\frac12}^{\frac32} \sup_{\Omega\in[\frac12,\frac32]} \Big|\frac{\partial}{\partial\Omega}e^{-Z\psi(\Omega)}\Big|d\Omega \\ &\le K_2 Z e^{-Z\psi_r(\frac12)}, \qquad K_2 = (1-2H)2^{2H},\end{aligned}$$

and

$$\Big|\mathrm{Re}\Big[\int_{\frac{3}{2}}^{\infty}\frac{1}{\Omega-1}e^{Z\Phi_s(\Omega,T)}d\Omega\Big]\Big| \le 2\int_{\frac{3}{2}}^{\infty}e^{-Z\psi_r(\Omega)}d\Omega$$
$$= 2e^{-Z\psi_r(\frac{3}{2})}\int_0^{\infty}e^{-Z[\psi_r(\frac{3}{2}+\Omega)-\psi_r(\frac{3}{2})]}d\Omega$$
$$\le K_3 e^{-Z\psi_r(\frac{3}{2})}, \qquad K_3 = 2\int_0^{\infty}e^{-[\psi_r(\frac{3}{2}+\Omega)-\psi_r(\frac{3}{2})]}d\Omega\,,$$

for any $Z \ge 1$. This shows that the integral from $1/2$ to ∞ is exponentially decaying in Z. The integral from $-\infty$ to $-1/2$ can be shown to be exponentially decaying in Z by a similar argument. This shows that the first integral of the lemma is exponentially decaying in Z.

Let us consider the second integral. We have

$$\Big|\mathrm{Re}\Big[\int_{\frac{1}{2}}^{\infty}e^{Z\Phi_s(\Omega,T)}d\Omega\Big]\Big| \le \int_{\frac{1}{2}}^{\infty}e^{-Z\psi_r(\Omega)}d\Omega$$
$$= e^{-Z\psi_r(\frac{1}{2})}\int_0^{\infty}e^{-Z[\psi_r(\frac{1}{2}+\Omega)-\psi_r(\frac{1}{2})]}d\Omega$$
$$\le K_4 e^{-Z\psi_r(\frac{1}{2})}, \qquad K_4 = \int_0^{\infty}e^{-[\psi_r(\frac{1}{2}+\Omega)-\psi_r(\frac{1}{2})]}d\Omega\,,$$

for any $Z \ge 1$. The integral from $-\infty$ to $-1/2$ can be shown to be exponentially decaying in Z by the same argument. This shows that the second integral of the lemma is exponentially decaying in Z. □

We can now consider the difference (67):

$$\Big|a(T,Z) - \frac{1}{\pi}\mathrm{Re}\Big[\int_0^{\infty}e^{Z\Phi_s(\Omega,T)}d\Omega\Big]\Big| \le \tilde{K}_1 e^{-\delta_H Z} + \frac{1}{2\pi}\int_{-\frac{1}{2}}^{\frac{1}{2}}\Big|1-\frac{1}{1-\Omega}\Big|e^{-Z\psi_r(\Omega)}d\Omega$$
$$\le \tilde{K}_1 e^{-\delta_H Z} + \frac{2}{\pi}\int_0^{\frac{1}{2}}\Omega e^{-Z\psi_r(\Omega)}d\Omega$$
$$\le \tilde{K}_1 e^{-\delta_H Z} + \tilde{K}_2 Z^{-\frac{2}{1-2H}}, \quad \tilde{K}_2 = \frac{2}{\pi}\int_0^{\infty}\Omega e^{-\psi_r(\Omega)}d\Omega\,.$$

This completes the proof of Lemma 6.1.

Appendix C. Analysis of the large-Y behavior of $A_s(Y)$ and $A_l(Y)$

Let us first address the short-range case $H < 1/4$ and denote

$$B_s(u) = \exp\big(-\exp\big(i\pi(H-1/2)\big)u^{1-2H}\big)\,.$$

We have

$$A_s(Y) = \frac{1}{\pi}\mathrm{Re}\Big[\int_0^{\infty}B_s(u)e^{-iuY}du\Big]\,.$$

We seek the large-Y behavior of $A_s(Y)$. General Abelian theorems indicate that it should be related to the small-u behavior of the function $B_s(u)$, thus, we write the function $B_s(u)$ in such a way that its small-u behavior can be clearly identified. Motivated by the expansion of the function $B_s(u)$ for small u, we write the function $B_s(u)$ in the form

$$B_s(u) = f_1\big([2H\cos(\pi(1/2-H))]^{\frac{1}{1-2H}}u\big) + if_2\big([\sin(\pi(1/2-H))]^{\frac{1}{1-2H}}u\big) + C_s(u)\,,$$

where f_1 and f_2 are defined by

$$f_1(u) = \Big(1 - \frac{1}{2H}u^{1-2H} + \frac{1-2H}{2H}u\Big)\mathbf{1}_{[0,1]}(u)\,, \tag{C1}$$

$$f_2(u) = \Big(u^{1-2H} - (1+2H)u + 2Hu^2\Big)\mathbf{1}_{[0,1]}(u)\,. \tag{C2}$$

Note that the linear and quadratic terms in the definitions of f_1 and f_2 have been added so that these functions are continuously differentiable over $(0,\infty)$ (even at $u=1$) and piecewise twice differentiable over $(0,\infty)$. The function $C_s(u)$ is continuously differentiable and piecewise twice differentiable over $(0,\infty)$, because B_s, f_1 and f_2 are continuously differentiable and piecewise twice differentiable over $(0,\infty)$. Moreover, C_s, C_s', and C_s'' are absolutely integrable over $(0,\infty)$, $C_s(0)=0$, and $C_s'(0^+)$ is well defined (here we use the fact that $2-4H>1$, so that the terms in u^{2-4H} that come from the expansions of the exponential are differentiable at zero). Consequently a double integration by parts yields:

$$\int_0^\infty C_s(u)e^{-iYu}du = -\frac{C_s'(0^+)}{Y^2} - \frac{1}{Y^2}\int_0^\infty C_s''(u)e^{-iYu}du \overset{Y\to\infty}{=} O\Big(\frac{1}{Y^2}\Big)\,. \tag{C3}$$

Moreover, by performing an integration by parts step, we obtain

$$\int_0^\infty f_1(u)e^{-iYu}du \overset{Y\to\infty}{\simeq} -\frac{i}{Y} + i\frac{1-2H}{2HY^{2-2H}}\int_0^\infty v^{-2H}e^{-iv}dv + o\Big(\frac{1}{Y^{2-2H}}\Big)\,,$$

$$\int_0^\infty f_2(u)e^{-iYu}du \overset{Y\to\infty}{\simeq} -i\frac{1-2H}{Y^{2-2H}}\int_0^\infty v^{-2H}e^{-iv}dv + o\Big(\frac{1}{Y^{2-2H}}\Big)\,.$$

The computation of the definite integral (see formula 3.761 in [15])

$$\int_0^\infty v^{-2H}e^{-iv}dv = \Gamma(1-2H)e^{-i(1-2H)\frac{\pi}{2}}\,, \tag{C4}$$

gives then

$$\mathrm{Re}\Big[\int_0^\infty f_1(u)e^{-iYu}du\Big] \overset{Y\to\infty}{\simeq} \frac{\Gamma(2-2H)}{2HY^{2-2H}}\sin((1-2H)\frac{\pi}{2}) + o\Big(\frac{1}{Y^{2-2H}}\Big)\,,$$

$$\mathrm{Re}\Big[i\int_0^\infty f_2(u)e^{-iYu}du\Big] \overset{Y\to\infty}{\simeq} \frac{\Gamma(2-2H)}{Y^{2-2H}}\cos((1-2H)\frac{\pi}{2}) + o\Big(\frac{1}{Y^{2-2H}}\Big)\,. \tag{C5}$$

Using (C3), (C5), and the identity

$$2\cos((1-2H)\frac{\pi}{2})\sin((1-2H)\frac{\pi}{2}) = \sin(2H\pi)\,,$$

we obtain the desired result.

If $H \in [1/4, 1/2)$, then one needs to consider the terms $u^{k(1-2H)}$, $1 \leq k \leq 1+\lfloor 1/(1-2H)\rfloor$, that come from the expansion of the exponential in the expression of $B_s(u)$ in the same way we have addressed u^{1-2H}. This gives corrective terms proportional to $Y^{-k(1-2H)-1}$ which are negligible compared to Y^{2H-2}.

The long-range case $H \in (1/2, 1)$ can be analyzed as the short-range case with $H \in (0, 1/4)$.

References

[1] J. Aaviksoo, J. Kuhl, and K. Ploog, *Observation of optical precursors at pulse propagation in GaAs*, Phys. Rev. A **44** (1991) 5353–5356.

[2] R. Albanese, J. Penn, and R. Medina, *Short-rise-time microwave pulse propagation through dispersive biological media*, J. Opt. Soc. Am. A **6** 1989) 1441–1446.

[3] R. Albanese, *Wave Propagation Inverse Problems in Medicine and Environmental Health*, in *Inverse Problems in Wave Propagation*, IMA Volume 90, edited by G. Chavent, G. Papanicolaou, P. Sacks, and W. Symes, Springer-Verlag (1997).

[4] L. Brillouin, *Uber die Fortpflanzung des Lichtes in dispergieren den Medien*, Ann. Phys. **44** (1914) 203–240.

[5] R. Burridge and H. W. Chang, *Multimode one-dimensional wave propagation in a highly discontinuous medium*, Wave Motion **11** (1989) 231–249.

[6] R. Burridge, G. Papanicolaou, and B. White, *One-dimensional wave propagation in a highly discontinuous medium*, Wave Motion **10** (1988) 19–44.

[7] N. A. Cartwright and K. E. Oughstun, *Uniform asymptotic applied to ultrawideband pulse propagation*, Siam Review **49** (2007) 628–648.

[8] J.-F. Clouet and J.-P. Fouque, *Spreading of a pulse traveling in random media*, Ann. Appl. Probab. **4** (1994) 1083–1097.

[9] S. Dolan, C. Bean, and B. Riollet, *The broad-band fractal nature of heterogeneity in the upper crust from petrophysical logs*, Geophys. J. Int. **132** (1998) 489–507.

[10] A. Fannjiang and K. Sølna, *Scaling limits for wave beams in atmospheric turbulence*, Stoch. Dyn. **4** (2004) 135–151.

[11] J.-P. Fouque, J. Garnier, G. Papanicolaou, and K. Sølna, *Wave propagation and time reversal in randomly layered media*, Springer, New York, 2007.

[12] A. E. Gargett, *The scaling of turbulence in the presence of stable stratification*, J. Geophys. Res. **93** (1988) 5021–5036.

[13] J. Garnier, *Solitons in random media with long-range correlation*, Waves Random Media **11** (2001) 149–162.

[14] J. Garnier and K. Sølna, *Pulse propagation in random media with long-range correlation*, SIAM Multiscale Model. Simul. **7** (2009) 1302–1324.

[15] I. S. Gradshteyn and I. M. Ryzhik, *Table of integrals, series, and products*, Academic Press, San Diego, 1980.

[16] A. Hanyga and V. E. Rok, *Wave propagation in micro-heterogeneous porous media: A model based on an integro-differential wave equation*, J. Acoust. Soc. Am. **107** (2000) 2965–2972.

[17] H. Jeong, A. Dawes, and D. Gauthier, *Direct observation of optical precursors in a region of anomalous dispersion*, Phys. Rev. Lett. **96** (2006) 143901.

[18] H. Jeong and U. Osterberg, *Coherent transients: optical precursors and* 0π *pulses*, J. Opt. Soc. Am. B. **25** (2008) B1–B5.

[19] H. Jeong and S. Du, *Two-way transparency in the light-matter interaction: Optical precursors with electromagnetically induced transparency*, Phys. Rev. A **79** (2009) 011802.

[20] D. Lukofsky, J. Bessette, H. Jeong, E. Garmire, and U. Osterberg, *Can precursors improve the transmission of energy at optical frequencies?*, Journal of Modern Optics **56** (2009) 1083–1090.

[21] R. Marty and K. Sølna, *Acoustic waves in long-range random media*, SIAM J. Appl. Math. **69** (2009) 1065–1083.

[22] X. Ni and R.R. Alfano, *Brillouin precursor propagation in the THz region in Lorentz media*, Optics Express **14** (2006) 4188–4194.

[23] K.E. Oughstun, *Dynamical evolution of the Brillouin precursor in RocardPowlesDebye model dielectrics*, IEEE Trans. on Antennas and Propagation **53** (2005) 1582–1590.

[24] E. J. G. Pitman, *On the behavior of the characteristic function of a probability distribution in the neighborhood of the origin*, J. Austral. Math. Soc **8** (1968) 422–443.

[25] P. Pleshko and I. Paloez, *Experimental observation of Sommerfeld and Brillouin precursors in the microwave domain*, Phys. Rev. Lett. **22** (1969) 1201–1204.

[26] C. Sidi and F. Dalaudier, *Turbulence in the stratified atmosphere: Recent theoretical developments and experimental results*, Adv. in Space Res. **10** (1990) 25–36.

[27] M. Sakai, R. Nakahara, J. Kawase, H. Kunugita, K. Ema, M. Nagai, and M. Kuwata-Gonokami, *Polariton pulse propagation at excitation resonance in CuCl: Polariton beat and optical precursor*, Phys. Rev. B **66** (2002) 33302.

[28] K. Sølna and G. Papanicolaou, *Ray theory for a locally layered medium*, Waves in Random Media **10** (2000) 151–198.

[29] K. Sølna, *Acoustic pulse spreading in a random fractal*, SIAM J. Appl. Math. **63** (2003) 1764–1788.

[30] A. Sommerfeld, *Uber die Fortpflanzung des Lichtes in dispergieren den Medien*, Ann. Phys. **44** (1914) 177–202.